Relocalization in Floppy Free Radicals: The OCNO and OCCHO Isoelectronic Series

A. L. Cooksy*

Contribution from the Department of Chemistry, San Diego State University, San Diego California 92182-1030

Received October 23, 2000

Abstract: A survey of the XCNY and XCCHY radicals with X and Y = CH_2, NH, and O has been carried out by ab initio QCISD/6-311G(d,p) calculations to assess the impact of low-lying excited electronic states on the molecular dynamics. Multiple canonical structures may be drawn for each of these structural formulas, with the principal competition for most stable configuration between a $^2A'$ form with four electrons in a'' orbitals and a $^2A''$ form with five a'' electrons. Other low-lying configurations may include a $5a''$ state with nominally pentavalent nitrogen and a $6a''$ state. Optimized geometries and harmonic frequencies were evaluated for the lowest-energy minima on the potential energy surfaces. Localized unpaired electron density causes the $4a''$ state to be the most stable for (NH)CCHO and OCCHY, whereas allylic resonance stabilization favors the $5a''$ state for all other radicals in the set. For five of the 18 molecules studied, secondary minima (excluding conformers) are found within 30 kJ mol^{-1} of the most stable state at the QCISD/6-311G(d,p) level, suggesting that photolysis or pyrolysis of parent compounds may result in multiple isomers of the resulting reactive intermediates. Predicted equilibrium geometries, approximate thermochemical quantities for dissociation of the central bond, and selected spectroscopic parameters are presented for all 18 structural formulas. Convergence tests were also performed for the glyoxallyl radical (OCCHO) to resolve discrepancies between single- and multireference post-SCF results. These tests find that extension of the MCSCF methods to include σ bonding orbitals or virtual-orbital CI brings MCSCF relative energies into agreement with results from standard single-reference CI and CC methods. Relative configurational energies evaluated at Hartree−Fock levels routinely differ from post-SCF values by 30 kJ mol^{-1} or more.

1. Introduction

The OCNO radical is the simplest of a family of XCNY and XCCHY radicals that includes the most stable isomers formed by hydrogen pyrolysis or photolysis of acrolein, 1,3-butadiene, methyl ketene, glyoxal, methyl isocyanate, and several basic unsaturated imines and amines. Interest in butadienyl as an intermediate in combustion, photochemistry, and interstellar chemistry has motivated its study by ESR spectroscopy, semiempirical methods, and ab initio computation.[1−7] The OCNO radical itself is a candidate intermediate in atmospheric reactions, and the subject of previous high-level calculations.[8] The lowest-energy configurational isomers of (CH_2)CCHO and OCCH(CH_2) have also been analyzed in detail.[9] However, the fundamental chemical link between these isoelectronic molecules has not been explored in previous studies.

These molecules also provide essential analogues with which to test computational approaches to dynamical problems in more complex systems, such as the cyclization of pentadienyl,[10,11] which to date has been probed with relatively low levels of theory. Previous calculations for butadienyl and its isomers suggest that a suitable choice of ab initio method may correct the predicted reaction enthalpies by as much as 60 kJ mol^{-1}.[7]

The XCNY and XCCHY radicals, with X and Y equal to CH_2, NH, or O, share a four-atom backbone bound by three σ bonds and a five-electron π system. On the basis of the canonical structures for these molecules, their chemical characteristics may be largely determined by a facile "relocalization" of the π electron density from one region of the molecule to another. A related form of this phenomenon has been extensively studied for planar $^2A'$ radicals in the HC_3O family.[12−14] Relocalization in HC_3O and its analogues also involve alterations in the distribution of a five-electron π system across a four-atom backbone, but there is no change in orbital symmetries along the isomerization coordinate. The OCNO radical and its analogues differ in that relocalization is accompanied by a change in the orbital symmetry plane of the unpaired electron. The electronic structures of the endpoints are consequently quite distinct: one offers allylic stabilization of the radical electron, and one provides conjugated π bonds. These configurations are

(1) Benson, S. W.; Haugen, G. R. *J. Phys. Chem.* **1967**, *71*, 1735−1746.
(2) Kaiser, R. I.; Stranges, D.; Lee, Y. T.; Suits, A. G. *Astrophys. J.* **1997**, *477*, 982−989.
(3) Kern, R. D.; Singh, H. J.; Wu, C. H. *Int. J. Chem. Kinet.* **1988**, *20*, 731−747.
(4) Callear, A. B.; Smith, G. B. *J. Phys. Chem.* **1986**, *90*, 3229−3237.
(5) Kühnel, W.; Gey, E.; Ondruschka, B. Z. *Z. Phys. Chem. (Leipzig)* **1987**, *268*, 23−32.
(6) Parker, C. L.; Cooksy, A. L. *J. Phys. Chem.* **1998**, *102*, 6186−6190.
(7) Parker, C. L.; Cooksy, A. L. *J. Phys. Chem.* **1999**, *103*, 2160−2169.
(8) Benson, B. D.; Francisco, J. S. *Chem. Phys. Lett.* **1995**, *233*, 335−339.
(9) Cooksy, A. L. *J. Phys. Chem.* **1998**, *102*, 5092−5099.
(10) Mare, G. R. D.; Deslauriers, H.; Collin, G. J. *Rsrch. Chem. Intermediates* **1990**, *14*, 133−159.
(11) Yamamoto, Y.; Ohno, M.; Eguchi, S. *J. Org. Chem.* **1996**, *61*, 9264−9271.
(12) Cooksy, A. L.; Tao, F.-M.; Klemperer, W.; Thaddeus, P. *J. Phys. Chem.* **1995**, *99*, 11095−11100.
(13) Cooksy, A. L. *J. Am. Chem. Soc.* **1995**, *117*, 1098−1104.
(14) Wang, H.; Cooksy, A. L. *Chem. Phys.* **1996**, *213*, 139−151.

10.1021/ja0037522 CCC: $20.00
Published on Web 04/07/2001

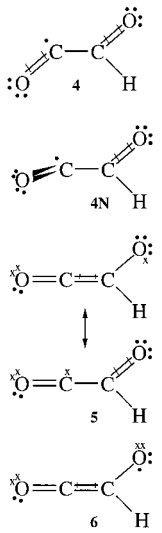

Figure 1. Principal canonical structures for the low-lying states of OCCHO. Crosses denote electrons in out-of-plane *a″* molecular orbitals.

drawn in Figure 1 for the glyoxallyl radical OCCHO and are identified by the number of electrons in out-of-plane *a″* symmetry molecular orbitals: four *a″* electrons for the conjugated π bond $^2A'$ configuration, and five *a″* electrons for an allylic $^2A''$ configuration. A second $^2A'$ configuration having six *a″* electrons is also drawn, this one with a central π orbital hyperconjugated to terminal lone pairs (or σ bonding orbitals).

Over the past decade, direct spectroscopic studies have begun to probe the molecular and electronic structures of radicals of this size with sufficient precision that analysis of the configurational dynamics is critical to interpretation of the data.[12] Simultaneously, the ab initio calculations have become tractable that can predict the isomerization surface connecting these configurations with an apparent accuracy of 5−10 kJ mol^{-1}. Nonetheless, recent studies on C_3H_3O[9] and C_4H_5[7] establish that discrepancies of more than 55 kJ mol^{-1} may arise between results predicted by different computationally intensive and presumably reliable methods; such disagreement was found between multireference and coupled cluster values for the 2-butynyl/cyclobutenyl relative energy, for example. These discrepancies are in sharp contrast to the excellent agreement among spectroscopic properties predicted by diverse levels of theory for the HC_3O[12] and HC_3NH[13] systems.

This report presents results from a series of calculations on these 18 XCNY and XCCHY radicals to assess the significance of the relocalization pathways on their intramolecular dynamics. An effort is also made to reconcile the discrepant relative energies found previously for the C_4H_5 and C_3H_3O isomers when comparing multi- and single-reference methods.

2. Methods

Reference wave functions were calculated at a variety of initial geometries for each molecule using the unrestricted Hartree−Fock (UHF) and restricted open-shell Hartree−Fock (ROHF)[15] approximations. The UHF wave functions suffer from spin contamination, although there is no evidence from previous studies of similar systems that this adversely affects the relative energies calculated using configuration interaction: agreement between single- and multireference results is excellent in the cases of HC_3O and HC_3NH, despite typical $\hat{S}^2$ expectation values of 1.2 for the UHF references.[14] The ROHF wave functions, while eigenfunctions of $\hat{S}^2$, neglect the breaking of the molecular orbital degeneracy in paramagnetic molecules and tend to overemphasize the stability of configurations with localized spin densities.[16]

Initial geometries were first based on the canonical structures drawn for the 4*a″*, 5*a″*, and 6*a″* electronic states of each species, examining all expected E- and Z- conformations for each state. The configuration 4 and 5 geometries were all initially optimized under C_s constraints; if the geometry was found to be unstable with respect to one of its vibrational coordinates, a second optimization was carried out from this optimized geometry slightly deformed in the direction of that coordinate. In any case, at least one additional calculation was carried out for each molecule from an initial C_1 geometry with nonplanar XCCY (or XCNY) backbone. When such a calculation converged to a C_1 geometry, the resulting structure could always be associated with either a nonplanar configuration 4 ("4N") or configuration 5 ("5N") on the basis of spin delocalization and bond angles.

The electronic structure of configuration 5 implies that when X is NH or CH_2, those hydrogens will be oriented perpendicular to the plane of the XCNY or XCCY backbone. Similarly, configuration 6 prefers both the X and Y group hydrogens to be perpendicular to the backbone plane. For methene, this still allows imposition of C_s symmetry constraints on the geometry and wave function, but when an N−H bond points out of the backbone plane, the C_s symmetry is broken. Configuration 5 is always sufficiently stable that this does not hinder identification of a corresponding minimum on the potential surface. For configuration 6, however, it was necessary to carry out partial optimizations in some cases, fixing the H-backbone dihedral angle to 90°.

The principal results cited are obtained using the size-consistent quadratic configuration interaction (QCISD) method.[17] This method, which may be written as a truncated form of the coupled cluster (CCSD) equations,[18] predicts relative energies and hyperfine constants for the C_4H_5 isomers and hyperfine and rotational constants for the similar HC_3O system usually to within the quoted experimental precision.[12,7] Furthermore, in extending the QCISD calculations to the CCSD(T) level, which incorporates an estimated contribution from triple substitutions, relative energies shift by less than the errors expected from neglect of anharmonicity in estimating the zero-point energies—that is, typically less than 2 kJ mol^{-1}.[12,14]

To explore the discrepancy between single- and multireference results found in C_3H_3O and C_4H_5, as well as to examine the accuracy of other approximations in this application, additional calculations were carried out on configurations 4 and 5 of OCCHO using perturbation theory (MP2 and MP4),[19,20] standard configuration interaction (CISD),[21] and CCSD(T) calculations, all based on the UHF reference wave functions. To test the influence of the reference wave function, CISD calculations were also carried out from the ROHF reference wave functions (ROCISD), with the set of external orbitals (unoccupied in the reference wave function) limited to 20 to expedite the numerical geometry optimizations.

(15) McWeeny, R.; Diercksen, G. *J. Chem. Phys.* **1968**, *49*, 4852−4856.
(16) Lepetit, M. B.; Malrieu, J. P.; Trinquier, G. *Chem. Phys.* **1989**, *130*, 229−239.
(17) Pople, J. A.; Head-Gordon, M.; Raghavachari, K. *J. Chem. Phys.* **1987**, *87*, 5968−5975.
(18) Purvis, G. D., III; Bartlett, R. J. *J. Chem. Phys.* **1982**, *76*, 1910−1918.
(19) Frisch, M. J.; Head-Gordon, M.; Pople, J. A. *Chem. Phys. Lett.* **1990**, *166*, 281−289.
(20) Krishnan, R.; Pople, J. A. *Int. J. Quantum Chem.* **1978**, *14*, 91−100.
(21) Raghavachari, K.; Pople, J. A. *Int. J. Quantum Chem.* **1981**, *20*, 1067−1071.

Multiconfiguration SCF (MCSCF)[22,23] calculations were also carried out for OCCHO, using complete active spaces ranging from five electrons in five orbitals (5,5) to all 21 valence electrons in 14 orbitals (21,14). The full valence active space employing 17 orbitals was not attainable with suitable basis sets, as the number of configuration space functions (CSF) in that limit exceeds 45 million, and integral storage for 1 million CSFs requires over 15 GB of disk space; in similar fashion, memory demands of the determinant CI method[24] exceed 10 GB for the full valence active space.

Active-space orbitals were normally selected from HF orbitals localized according to Pipek and Mizey's scheme,[25] including those occupied orbitals with the greatest π and unpaired electron character. Localized orbitals simplify the selection of the active space in these cases without affecting the variational energy. Virtual orbitals from the HF reference were chosen to yield the lowest variational single-point MCSCF energy; these were always found to be a set such that each doubly occupied orbital in the HF reference was matched by a virtual orbital of the same symmetry representation. The (7,7) and (9,9) MCSCF wave functions were used as references for multireference CISD (MRCISD) and MP2 (MCMP2) calculations.[26,27] The most computationally demanding calculations were MRCISD calculations based on an MCSCF(7,7) reference that included all single and double substitutions into 43 external orbitals.

Geometries were optimized for the OCCHO configurations 4 and 5 at all levels of theory save MCSCF(21,14) and MRCISD, and for the Z-conformer of configuration 4 ("4Z") at all but the largest MP, CI, and MCSCF levels. Relative UHF energies differ by less than 5 kJ mol^{-1}across the range of CI and MCSCF optimized geometries found, and restriction of the MCSCF(21,14) and MRCISD calculations to fixed geometries is expected to introduce errors no greater than this. The nonplanar configuration 4N need not be a stationary point on the vibrational potential energy surface, and optimized geometries are reported for 4N only at those levels where it was found to be a minimum.

Pople's 6-311G(d,p)[28,29] basis set was employed for the majority of the calculations and was often checked by comparison to results obtained with Dunning's cc-pVTZ basis.[30] The cc-pVTZ basis comprises 120 contracted functions for OCNO and 134 for OCCHO, compared to 72 and 78, respectively, for the 6-311G(d,p) basis, and it expands the polarization functions to include contributions of f symmetry. The QCISD/cc-pVTZ relative energies differ by less than 8 kJ mol^{-1} from the 6-311G(d,p) relative energies for OCNO and OCCHO, and the harmonic frequencies all agree to within 11 cm^{-1}. In an effort to test for significantly larger basis set effects in the remaining species, all of the UHF/6-311G(d,p) optimized geometries were optimized again at the UHF/cc-pVTZ level and were found to predict relative energies within 10 kJ mol^{-1} of the 6-311G(d,p) values. Because a nearly 8 kJ mol^{-1} shift in relative energy was seen for configuration 4 of OCCHO upon expanding the basis set, further single-point energy calculations were carried out at the QCISD/cc-pVQZ level (250 contracted functions) for configurations 4, 4N, and 5. The resulting energies differ by less than 0.4 kJ mol^{-1} from the cc-pVTZ values. The adequacy of the 6-311G(d,p) basis set is further supported by experimental corroboration of the HC_3O geometry, hyperfine constants,[31] and observed vibrational frequency[32] predicted at the QCISD/6-311G(d,p) level.[12] In a systematic study, Wong and Radom also concluded that QCISD/6-311G(d,p) calculations adequately predict the geometries and energetics of alkene-radical reactions.[33]

Harmonic vibrational frequencies were calculated for all UHF and ROHF structures, and for the most stable QCISD structures. Vibrational analysis was generally omitted at the QCISD level for configurations found to lie above 50 kJ mol^{-1} and having imaginary frequencies at the HF level.

Bond dissociation energies (BDEs) were estimated for each of the 18 molecules by comparing the QCISD energy of the most stable configuration to the QCISD energies of the separated components. All dissociation energies are estimated for dissociation into the spin doublet and singlet fragments, including the vinylidene fragment (CCH_2) which has a nearly isoenergetic triplet state.

All multireference (MCSCF and MRCI) and ROCISD calculations were carried out using the Gamess programs;[34] all other calculations employed Gaussian 98.[35] The calculations were performed on a variety of Compaq and Silicon Graphics workstations, and a Cray C916.

3. Results and Discussion

On the basis of the present OCCHO studies and previous C_4H_5 and C_3H_3O studies, the QCISD method appears to be capable of predicting CCSD(T) relative energies within 5 kJ mol^{-1} or better, and the CISD results agree to within about 10 kJ mol^{-1}. While spin contamination causes $\langle S^2 \rangle$ values to extend as high as 1.647 for methods based on a UHF reference wavefunction, nearly all of the configurations within 50 kJ mol^{-1} of the most stable have $\langle S^2 \rangle$ values below 1.3, and values of 0.9 or below when quartet spin contributions are projected out of the wavefunction.

For simplicity, when the geometries optimize to C_1 or C_{2v} symmetry, the configurations will continue to be labeled "4", "5", and "6" in accord with the number of a'' electrons associated with the most closely related C_s structure. The distinction between these structures is then based on the following characteristics of the canonical forms:

• Configuration 4 is typified by a backbone with X═C−C═Y (or X═C−N═Y) bond order pattern and unpaired electron

(22) Werner, H.-J. *Adv. Chem. Phys.* **1987**, *69*, 1−62.
(23) Shepard, R. *Adv. Chem. Phys.* **1987**, *69*, 63−200.
(24) Knowles, P. J.; Handy, N. C. *Chem. Phys. Lett.* **1984**, *111*, 315−321.
(25) Pipek, J.; Mezey, P. Z. *J. Chem. Phys.* **1989**, *90*, 4916−4926.
(26) Brooks, B. R.; Laidig, W. D.; Saxe, P.; Handy, N. C.; H. F. Schaefer, I. *Phys. Scr.* **1980**, *21*, 312−322.
(27) Nakano, H. *J. Chem. Phys.* **1993**, *99*, 7983−7992.
(28) Krishnan, R.; Binkley, J. S.; Seeger, R.; Pople, J. A. *J. Chem. Phys.* **1980**, *72*, 650−654.
(29) Frisch, M. J.; Pople, J. A.; Binkley, J. S. *J. Chem. Phys.* **1984**, *80*, 3265−3269.
(30) T. H. Dunning, J. *J. Chem. Phys.* **1989**, *90*, 1007−1023.
(31) Cooksy, A. L.; Watson, J. K. G.; Gottlieb, C. A.; Thaddeus, P. *J. Chem. Phys.* **1994**, *101*, 178−186.
(32) Jiang, Q.; Graham, W. R. M. *J. Chem. Phys.* **1993**, *98*, 9251−9255.
(33) Wong, M. W.; Radom, L. *J. Phys. Chem.* **1995**, *99*, 8582−8588.
(34) Schmidt, M. W.; Baldridge, K. K.; Boatz, J. J.; Elbert, S. T.; Gordon, M. S.; Jensen, J. H.; Koseki, S.; Matsunaga, N.; Nguyen, K. A.; Su, S. J.; Windus, T. L.; Dupois, M.; Montgomery, J. A. *J. Comput. Chem.* **1993**, *14*, 1347−1363.
(35) Frisch, M. J.; Trucks, G. W.; Schlegel, H. B.; Scuseria, G. E.; Robb, M. A.; Cheeseman, J. R.; Zakrzewski, V. G.; Montgomery, J. A., Jr.; Stratmann, R. E.; Burant, J. C.; Dapprich, S.; Millam, J. M.; Daniels, A. D.; Kudin, K. N.; Strain, M. C.; Farkas, O.; Tomasi, J.; Barone, V.; Cossi, M.; Cammi, R.; Mennucci, B.; Pomelli, C.; Adamo, C.; Clifford, S.; Ochterski, J.; Petersson, G. A.; Ayala, P. Y.; Cui, Q.; Morokuma, K.; Malick, D. K.; Rabuck, A. D.; Raghavachari, K.; Foresman, J. B.; Cioslowski, J.; Ortiz, J. V.; Stefanov, B. B.; Liu, G.; Liashenko, A.; Piskorz, P.; Komaromi, I.; Gomperts, R.; Martin, R. L.; Fox, D. J.; Keith, T.; Al-Laham, M. A.; Peng, C. Y.; Nanayakkara, A.; Gonzalez, C.; Challacombe, M.; Gill, P. M. W.; Johnson, B. G.; Chen, W.; Wong, M. W.; Andres, J. L.; Head-Gordon, M.; Replogle, E. S.; Pople, J. A. *Gaussian 98*, revision A.6; Gaussian, Inc.: Pittsburgh, PA, 1998.

Table 1. Comparison of OCCHO Properties Predicted by Different Methods[a]

	$\Delta E(5-4N)$ (kJ mol^{-1})	$r_{CC}(5)$ (Å)	$r_{CC}(4)$ (Å)	$r_{CC}(4N)$ (Å)	$\mu_a(5)$[b] (D)	$\mu_a(4N)$[b] (D)	$\nu_1(5)$ (cm^{-1})
			6-311G(d,p)				
ROHF	13.3	1.362	1.547	1.521	1.79	2.24	152
UHF	−7.6	1.370	1.553	1.488	1.87	2.21	266
B3LYP		1.391	1.591	n.s.	1.94	n.s.	182
MP2	18.3	1.410	1.572	1.566	1.96	1.80	191
MP4(SDTQ)	14.2	1.413	1.599	1.584	1.93	1.87	
CISD	−0.1	1.388	1.562	1.531	1.89	2.02	230
ROCISD	11.6	1.427	1.589	1.546	2.21	2.26	
QCISD	3.3	1.401	1.583	1.522	1.83	1.86	183
CCSD(T)	3.2	1.405	1.586	1.528	1.87	1.87	
MCSCF(9,9)	21.9	1.386	1.527	1.510	1.53	1.95	63
MCSCF(11,11)	20.2	1.395	1.546	1.520	1.62	1.94	
MCSCF(21,14)[c]	−3.4						
MCMP2(9,9)	−8.2	1.386	1.607	1.498	2.54	2.15	
			QCISD				
4-31G	−0.6	1.390	1.568	1.455	2.04	2.11	106
6-31G	2.9	1.397	1.562	1.484	2.07	2.15	87*i*
6-31G(d,p)	4.8	1.397	1.566	1.511	1.94	1.99	
cc-pVDZ	3.6	1.410	1.583	1.523	1.98	1.77	150
6-311G(d,p)	3.3	1.401	1.583	1.522	1.83	1.86	183
6-311++G(2df,2p)	−3.6	1.393	1.566	1.486	n.s.	2.03	
cc-pVTZ	−1.4	1.394	1.573	1.496	1.99	1.94	
cc-pVQZ[d]	−1.7						

[a] No values are provided for structure 4N for calculations where it is not a stationary point. [b] Values of dipole moment μ quoted for the ROCISD, MCMP2, CCSD(T), and MP4(SDTQ) levels are calculated at those optimized geometries using the CISD, MP2, QCISD, and MP4(SDQ) methods, respectively. [c] Energy evaluated at the MCSCF(11,11)/6-311G(d,p) optimized geometry. [d] Energy evaluated at the QCISD/cc-pVTZ optimized geometry.

density highly localized on the second atom of the backbone. When the backbone is planar, this permits conjugation between the two π bonds.

- An allylic 3-electron, 3-center distribution stabilizes configuration 5, lending partial double bond character to the X−C and C−C (or C−N) bonds.
- To achieve configuration 6, a central π bond is conjugated to lone pair or σ-bonding electrons at the X and Y termini.

Geometries and relative energies are more strongly determined by the X substituent than the Y, and discussions of specific molecules are therefore grouped by X below.

3.1. Analysis of Methods. Table 1 lists properties for OCCHO obtained from a wide range of geometry optimizations. Depending on level of theory and basis set, the OCCHO minima are distributed among configurations 4, 4Z, 4N, and 5. Zero-point corrections to these relative energies are 2.7 kJ mol^{-1} or less for all but one level of theory: the MP2 calculations for configurations 4 and 4Z predict unrealistically high CO stretching frequencies of over 3500 cm^{-1}, raising the zero-point correction to over 5.5 kJ mol^{-1}. The error arises principally from a value of 4.8×10^6 dyn cm^{-1} for the formyl CO diagonal element of the force constant matrix, roughly 3 times the expected value. This effect appears regardless of symmetry constraints and is still present when the cc-pVTZ basis set is used.

As the CC bond lengths in Table 1 indicate, the optimized geometries are consistent with the canonical structures in Figure 1; the CC single/double bond of resonant configuration 5 ranging between 1.36 and 1.41 Å and the formal single bond of configuration 4 longer by 0.15 to 0.22 Å. The CC bond lengths predicted for configuration 4N are shorter than those of configuration 4 by 0.02−0.07 Å, consistent with limited conjugation of the unpaired electron and a CO π bond. The ROHF and UHF optimized geometries differ from those predicted at correlated levels of theory primarily in having CO and CC bond lengths about 0.02 Å smaller. The geometric parameters most sensitive to level of theory are the CC bond length in configuration 4, which varies from 1.53 Å in the MCSCF calculations to 1.61 in the MCMP2 optimization, and the configuration 4N ketenyl CCO bond angle, which varies from 124.0° at MP2 to 139.1° at UHF. Bond angles across all levels of theory otherwise vary less than 6°. Predicted equilibrium dihedral OCCO angles for configuration 4N are all within 14° of 90°.

Spin density analyses at all levels of theory except MP2 were consistent with a nearly equal representation of the two resonance structures drawn for configuration 5, splitting the spin density across the ketenyl carbon and formyl oxygen atoms, and were consistent with single canonical forms for configurations 4, 4Z, and 4N, localizing the spin density near the ketenyl carbon.

The lower section of Table 1 illustrates that predicted values of the geometric parameters are well-converged with respect to basis set. Once the basis set is extended to at least 40 contracted functions (beyond 6-31G), bond lengths differ by less than 0.035 Å at the QCISD level. In contrast, the relative energies listed in Table 1 for various levels of theory are remarkably inconsistent, even in predicting which configurations are minima on the potential surface. Configuration 5 is the most stable configuration according to the UHF and B3LYP calculations, whereas it is 22 kJ mol^{-1} less stable than 4 at the MCSCF(9,9) level. Configuration 4N is the most stable according to the MP, QCISD, and CCSD(T) calculations but is not a minimum at the B3LYP or small active-space MCSCF levels.

The distinction of being the most stable of three nearly isoenergetic configurations needs not carry any dramatic experimental consequences. In the case of OCCHO, however, if one neglects the low-level ROHF, UHF, B3LYP, MP2, and MCSCF(5,5) results, the remaining levels of theory present significantly distinct conclusions: (1) For the single-reference calculations, configuration 4N is consistently the most stable when zero-point corrections are included; more stable than 4 by 8−10 kJ mol^{-1} and more stable than 5 by 3−14 kJ mol^{-1}; (2) for the multireference calculations, configuration 4 is most

Table 2. Values of C_0^2 for Multireference and $\langle S^2 \rangle$ for Single-Reference OCCHO Wave Functions

	configuration			
	5	4	4Z	4N
active space		C_0^2 at 6-311G(d,p)		
(5,5)	0.93	0.89	0.83	n.s.
(7,7)	0.90	0.88	0.82	n.s.
(9,9)	0.90	0.87	0.82	0.90
(11,11)	0.89	0.87		0.90
level		$\langle S^2 \rangle$ at 6-311G(d,p)		
UHF	0.839	0.772	0.775	0.833
B3LYP	0.759	0.753	0.753	n.s.
MP2	0.845	0.777	0.779	0.782
MP4(SDTQ)	0.852	0.781		0.784
CISD	0.842	0.775	0.779	0.799
QCISD	0.853	0.805	0.823	0.842
CCSD(T)	0.855	0.807		0.842
basis		$\langle S^2 \rangle$ at QCISD		
4-31G	0.910	1.230	1.075	1.059
6-31G	0.916	1.271	1.096	1.117
6-31G(d,p)	0.858	0.834	0.858	0.866
cc-pVDZ	0.857	0.815	0.837	0.855
6-311G(d,p)	0.853	0.805	0.823	0.842
6-311++G(2df,2p)	0.844	0.789		0.858
cc-pVTZ	0.847	0.787		0.854
cc-pVQZ	0.847	0.798		0.854

stable; more stable than 5 by 10−20 kJ mol^{-1}, and 1−3 kJ mol^{-1} more stable than 4N at MCSCF levels. The ROHF, B3LYP, and MP2 levels which are neglected in these conclusions were also found to be the least reliable in Wong and Radom's study of similar-sized radical systems.[33] They found that B3LYP sporadically exhibited large errors, and that unrestricted MP2 predictions suffered more from spin contamination than even the UHF reference values. While ROHF is immune to spin contamination, its consistently high variational energies relative to UHF indicate a comparative weakness in modeling the multielectron wave function, and MCSCF with small active spaces may do little to correct this failing.

Nonetheless, spin contamination in the OCCHO single-reference calculations is large, with the $\langle S^2 \rangle$ values in Table 2 between 0.753 and 0.855. In addition, the contribution C_0^2 of the single-reference HF wave function to the MCSCF wave function is usually 90% or less. These suggest that a multi-reference method based on restricted HF wave functions may be valuable in the assessment of the molecular properties.

However, nearly all the MCSCF correlation energy is recovered in the single and double substitutions. The most significant contribution from triple substitutions of the HF reference in the MCSCF space occurs in the MCSCF(9,9) wave function for configuration 4N, in which the triples amount to approximately 0.8% of the overall probability density. Furthermore, the multireference calculations neglect substantial contributions to the correlation energy from substitutions involving occupied and virtual orbitals not included in the active space; the absolute energies at the MCSCF(11,11) level are 0.38 hartree higher than the CISD absolute energies, and only 0.17 hartree lower than the UHF energies. Single and double substitutions of the 21 valence electrons into the 20 lowest unoccupied orbitals of the reference is sufficient to recover more than half of the difference between UHF and CISD energies.

Finally, comparison of the multireference results is complicated by the difference in electronic structure between configurations 4 and 5. For example, optimal selection of the (5,5) active space for configuration 5 samples three a'' out-of-plane orbitals, representing the allylic system of orbitals, and two a' orbitals, corresponding to the ketene CO π and π^*. The configuration 4 active space samples four a'' orbitals, representing the conjugated out-of-plane π system, and a single in-plane a' orbital. The degree of conjugation is not the same in the two configurations, and this is likely to impact the amount of correlation energy recovered in each case.

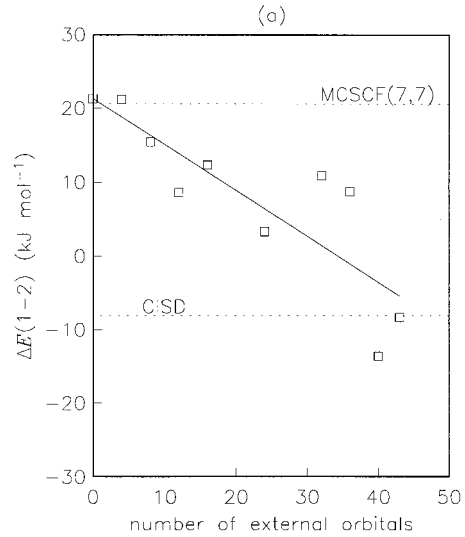

Figure 2. MRCISD(7,7,*n*) relative energies of the OCCHO configurations 4 and 5 plotted as a function of the number *n* of external orbitals used. Dashed lines represent the energies calculated at MCSCF(7,7) and CISD levels.

Post-ROHF and post-MCSCF methods were employed to assess the influence of these factors. The ROCISD and MCMP2 results cited in Table 1 reduce the relative energy of configuration 5 from the ROHF and MCSCF values. However, these energies and certain geometric parameters—for example, $r_{CC}(5)$ for ROCISD and $r_{CC}(4)$ for MCMP2—are still in poor agreement with the evidently well-converged QCISD and CCSD(T) values, and they leave in doubt the adequacy of the ROHF reference at the present level of CI and the effectiveness of MP2 for these systems. Wong and Radom found restricted MP2 predictions to be substantially improved over UMP2, but still preferred QCISD overall.[33]

Multireference CISD calculations normally provide excellent wave functions, and also allow a comparison of influences of the different contributions to the full CI expansion offered by the MCSCF and CISD truncations. The MRCISD relative energy $E(5-4)$ of configuration 5 relative to 4 obtained as a function of external orbital number *n* is plotted in Figure 2. The plot clearly shows the 5−4 relative energy approaching the CISD value as *n* climbs, reaching the CISD value as *n* exceeds 40. (The maximum number of external orbitals for this basis set and active space is 64.) The MCSCF(7,7) wave function was used as a reference, because single point relative energies calculated at this level were in qualitative agreement with those obtained using the (9,9) and (11,11) active spaces. Although configuration 4N is not a local minimum on the potential surface at the MCSCF(7,7) level, the (7,7) relative energy $E(5-4)$ obtained at the (11,11) optimized geometries is 4.2 kJ mol^{-1}, in excellent agreement with the 3.1 kJ mol^{-1} value obtained at the MCSCF(11,11) level.

However, addition of single and double substitutions to the MCSCF(7,7) wave functions did not show any tendency to change the relative energy of configurations 4 and 4N. Single-point MRCISD calculations were carried out with up to 24 external orbitals for configuration 4N (the lack of symmetry in configuration 4N reduces the number of external orbitals

Table 3. QCISD/6-311G(d,p) Central Bond Dissociation Energies and Entropies

	ΔE (kJ mol^{-1})	ΔS (J K^{-1} mol^{-1})		ΔE (kJ mol^{-1})	ΔS (J K^{-1} mol^{-1})
OCNO	−162	130	OCCHO	−46	138
OCN(NH)	−92	147	OCCH(NH)	3	155
OCN(CH_2)	9	141	OCCH(CH_2)	55	147
(NH)CNO	−97	130	(NH)CCHO	41	145
(NH)CN(NH)	−39	147	(NH)CCH(NH)	94	147
(NH)CN(CH_2)	58	148	(NH)CCH(CH_2)	138	149
(CH_2)CNO	166	150	(CH_2)CCHO	249	159
(CH_2)CN(NH)	156	172	(CH_2)CCH(NH)	314	167
(CH_2)CN(CH_2)	253	169	(CH_2)CCH(CH_2)	362	169

available for given computational resources). A remaining weakness of the MCSCF wave function is the neglect of substitutions from those valence orbitals not belonging to the active space. The MCSCF(11,11) calculations employ 11 valence electrons in constructing the configuration space, but this leaves 10 valence electrons in their original HF orbitals. Single-point calculations were therefore carried out with a (21,14) active space, which considered all the valence electrons for each configuration, although the number of orbital configurations was limited by the use of only three virtual orbitals from the HF reference. These calculations considered roughly 91 000 orbital configurations for configuration 5, compared to some 580 000 orbital configurations treated in the maximum MRCISD calculations. The relative energies achieved in these calculations were $\Delta E(5-4) = -11.5$ kJ mol^{-1}, $\Delta E(4N\text{-}4) = -8.1$ kJ mol^{-1}. These values are in good agreement with the CISD relative energies of −8.1 and −7.9 kJ mol^{-1}, respectively, and are also in fair agreement with the QCISD and CCSD(T) relative energies in Table 1.

The QCISD predictions are therefore offered as the principal results of the present work, based on their history of excellent agreement with experimental data when available[7,12,33] and the eventual concurrence of the extended multireference methods described above. Examining the results for the entire set of molecules, the HF methods remain adequate for estimating these relative configurational energies to within about 30 kJ mol^{-1}, but vary from the QCISD results in one principal regard. As noted previously,[12] the correlation energy correction in these systems tends to be greater for geometries away from the minima. As a result, the barriers between adjacent configurations at the HF levels are often smoothed away entirely in the QCISD calculations. Therefore, the HF methods tend to overestimate the number of local minima that appear on the higher-level surfaces. Where isomerization barriers remain, the HF calculations may be expected to be overestimate them by several kJ mol^{-1}.

There is no evident correlation among the worst discrepancies between the UHF and QCISD relative energies; the cases where the discrepancy exceeds 30 kJ mol^{-1} are (CH_2)CNO 4, (CH_2)CNO 5, (CH_2)CN(NH) 6, and OCCHO 6. Where UHF and ROHF results diverge, the UHF usually gives better agreement with the QCISD.

Out of all the UHF and QCISD calculations, the zero-point corrections alter the relative energies by 5−7 kJ mol^{-1} in three cases (without affecting the energy ordering of the configurations). In all other cases the relative energies are corrected by less than 5 kJ mol^{-1}, typically by 2−3 kJ mol^{-1}.

3.2. Dissociation. Predicted energies (including zero-point energy corrections) and entropies for dissociation of the central bond in the most stable configuration are tabulated in Table 3

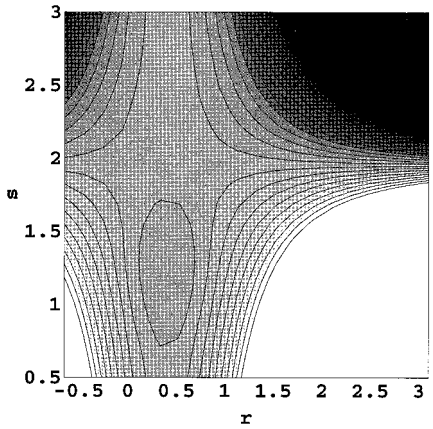

Figure 3. Contour plot of the potential energy surface for 5*a*″ OCNO. The parametric coordinates *r* and *s* are chosen such that r_{CN} is the distance from the origin (Å) and θ_{CNO} is the angle measured from the *r* axis toward the *s* axis. The contour spacing is 10 kJ mol^{-1}, with increasing darkness indicating lower energy.

for each molecule. Five of the 18 molecules—OCCHO, (NH)CN(NH), (NH)CNO, OCN(NH), OCNO—are predicted to be less stable than the dissociated fragments, and OCN(CH_2) is not significantly more stable than its daughter fragments. Four of the molecules—(CH_2)CCHO, (CH_2)CN(CH_2), (CH_2)CCH(NH), and (CH_2)CCH(CH_2)—have dissociation energies over 200 kJ mol^{-1}. To generalize, the CN central bond is substantially weaker than an otherwise equivalent CC central bond, and the central bond weakens further as the electronegativities of the X and Y groups increase. Predicted ΔS values for dissociation range from 130 to 172 J K^{-1} mol^{-1}.

The Table 3 BDEs are not expected to be as accurate as the relative configurational energies discussed below. In their study of the OCNO radical, Benson and Francisco found a 14 kJ mol^{-1} drop in dissociation energy when an estimated triple substitutions contribution was added to the QCISD values, and an additional 21 kJ mol^{-1} decrease with expansion of the basis set from 6-311G(2d,2p) to 6-311G(3df,3pd).[8] Our own calculations find that the BDE of OCCHO decreases from 46 to 22 kJ mol^{-1} on expansion of the basis set from 6-311G(d,p) to cc-pVQZ. Our previous estimate of the butadienyl enthalpy of formation, based on similar methods, was 14 kJ mol^{-1} below the experimental value.[7] Therefore, while qualitative trends are probably reliable, the Table 3 BDEs are expected to be accurate only to within about 40 kJ mol^{-1}.

Although the central OCNO bond dissociates with greater exothermicity than any of the other radicals studied, it is not obvious that this dissociation would most easily proceed along the $^2A''$ potential surface of the ground 5*a*″ state. The vibrational surface of configuration 4 connects to that of 5 via the sequential out-of-plane bending of the OCN angle and torsion about the CN bond. Configuration 4 has an electron distribution more closely resembling the CO and NO fragments than does configuration 5, and may be the more facile route for dissociation. While the thermochemistry of this dissociation was analyzed by Benson and Francisco, the scope of their study did not include the mechanism for dissociation.[8]

Energies were evaluated for 37 points on the OCNO potential energy surface for optimized geometries with fixed CN bond lengths and OCN bond angles at the QCISD/6-311G(d,p) level (Figure 3). From these calculations, we estimate the transition state on the $^2A''$ potential energy surface to lie at a CN bond length of 1.5 Å and CNO bond angle of 150° atop an energy barrier of roughly 35 kJ mol^{-1} (uncorrected for zero-point

Table 4. Relative Energies (kJ mol^{-1}) of the Most Stable XCNY and XCCHY Configurations[a]

	config	UHF	ROHF	QCISD		config	UHF	ROHF	QCISD
OCNO	4		(dissociates)		OCCHO	4	[15.8]	1.8	[9.2]
	5	0	0	0		4N	7.6	0	0
	6	19.6	16.5	27.5		5	0	12.8	3.3
OCN(NH)	4	106.0	[107.6]	[76.9]		6	125.1	109.6	172.6
	5	0	0	0	OCCH(NH)	4	13.5	0	0
	6	[24.0]	[21.1]	[28.1]		5	0	2.7	4.8
OCN(CH_2)	4	83.2	80.5	[63.5]		6	[127.5]	[60.3]	(137.1)
	5	0	0	0	OCCH(CH_2)	4	1.9	0	0
	6	[3.5]	[5.0]	[8.2]		5	0	[35.0]	7.6
(NH)CNO	4	66.5	90.1	(58.7)		6	[38.2]	[35.0]	(52.5)
	5	21.9	[22.2]	0	(NH)CCHO	4	3.1	0	[9.7]
	5N	0	0	-		4N	0	4.3	0
	6	[52.0]	[52.4]	(75.5)		5	[51.3]	65.0	[56.4]
(NH)CN(NH)	4	64.5	74.6	[57.0]		6		(converges to 4N)	
	5	[34.3]	[35.4]	[18.8]	(NH)CCH(NH)	4	6.7	0	[7.8]
	5N	0	0	0		4N	0	17.2	0
	6		(converges to 5N)			5	[63.7]	[72.6]	(67.4)
(NH)CN(CH_2)	4	[48.8]	46.8	[41.5]		6	[137.1]	[60.7]	(139.6)
	5	[23.2]	[21.5]	[23.4]	(NH)CCH(CH_2)	4	[11.6]	0	[4.8]
	5N	0	0	0		5	[75.1]	[76.0]	(72.6)
	6	[23.0]	[23.4]	[26.9]		5N	0	12.0	0
(CH_2)CNO	4	[58.6]	81.0	(106.9)		6	[51.4]	[39.3]	(53.3)
	5L	0	10.3	0.0	(CH_2)CCHO	4	3.8	43.8	12.8
	5	20.2	0.0	86.8		5	0	[60.2]	0
	6		(converges to 5L)			6	90.9	71.1	(105.2)
(CH_2)CN(NH)	4	22.9	46.5	42.9	(CH_2)CCH(NH)	4	14.0	0	[25.0]
	5	0	0	0		5	0	10.5	0
	5L	[96.4]	[103.8]	(53.1)		6	[76.1]	[38.9]	[76.1]
	6		(converges to 5L)		(CH_2)CCH(CH_2)	4	[16.9]	1.2	[35.0]
(CH_2)CN(CH_2)	4	[16.5]	[20.0]	[33.1]		5	0	0	0
	5	0	0	0		6	[69.2]	[29.1]	(55.2)
	6	[53.4]	[48.5]	(54.1)					

[a] All results using 6-311G(d,p) basis set, zero-point corrections not included. Square brackets denote a saddle point configuration; parentheses indicate that no vibrational analysis was performed.

motion). Eleven additional geometries were optimized for fixed values of the OCNO dihedral angle and CNO bond angle to search for a lower-energy threshold onto the dissociating 4a″ surface. This threshold appears upon excitation of the out-of-plane bend at energies above about 15 kJ mol^{-1}, and is likely therefore to be the dominant pathway for dissociation. In either case, few vibrational levels are likely to be bound by this shallow dissociation barrier (the combined harmonic zero-point energy in the dihedral and OCN bending motions is 3.5 kJ mol^{-1}), and the lifetime of OCNO may be expected to be short at any but the lowest temperatures.

Although OCN(CH_2) is predicted be more stable than its fragments by nearly 10 kJ mol^{-1}, this is less than the expected error in these estimates. Furthermore, the entropy favors dissociation by 140 J K^{-1} mol^{-1}, reducing the standard free energy of dissociation to −33 kJ mol^{-1} at 298 K.

The six radicals that dissociate to form vinylidene account for the six largest dissociation energies in Table 3. However, the subsequent isomerization of vinylidene to acetylene would improve the stability of the fragments by an additional 171 kJ mol^{-1} at this level of theory.

3.3. Configurational Energies. 3.3.1. Summary. The relative energies obtained at HF and QCISD levels for the most stable conformers of each configuration are reported in Table 4, and minimum energy configurations lying within 40 kJ mol^{-1} of the most stable form are drawn in Figure 4. When there exist saddle point C_s conformers of more stable nonsymmetric structures, both are listed in the table as, for example, configurations 5 and 5N, respectively. Configuration 6 imine radicals, which generally converge to non-C_s geometries, are excepted from this rule because the constrained C_s structures are much higher in energy.

Single bond torsions to form less stable Z or E conformers tend to increase the relative energy by 3−4 kJ mol^{-1}, although there are three cases in which the configuration 4 Z−E relative energy lies in the 10−20 kJ mol^{-1} range: OCCHO, (NH)CCHO, and (NH)CN(CH_2). For (NH)CCH(NH) 4 and (CH_2)CCH(NH) 4 and 5, the Z conformers for the CH−N−H bond system are slightly more stable than the corresponding E conformers.

The Hartree−Fock results place configuration 4 more than 50 kJ mol^{-1} above configuration 5 for the XCNOs, OCNYs, and (NH)CN(NH). On the other hand, while 5 remains more stable at the UHF level, 4 is the most stable configuration for the (NH)CCHY and OCCHY molecules at QCISD and ROHF levels. Characteristics that may contribute to the stability of this form are conjugation of the X−C and C−Y π-bonds and localization of the unpaired electron in an sp^2-type MO on the carbon atom adjacent to X. An especially electronegative X substituent borrows charge density from the neighboring carbon atom, which is partially restored by a highly localized unpaired electron MO with significant s-character.

Configuration 4N, the version of configuration 4 with a 90° torsion about the central single bond, accounts for the most stable geometries of OCCHO (at the ROHF and QCISD levels) and (NH)CCH(NH) and (NH)CCHO (at the UHF and QCISD levels). The relative stability of this nonplanar form apparently improves with increasing electronegativity of the end groups, and indicates that the π-bond conjugation is often subordinate to the spin localization in determining stability. In these cases, the planar form is in any event predicted to lie less than 10 kJ mol^{-1} higher in energy, and the spin density is more delocalized in the nonplanar form than in the planar through partial conjugation with the C−Y bond MOs.

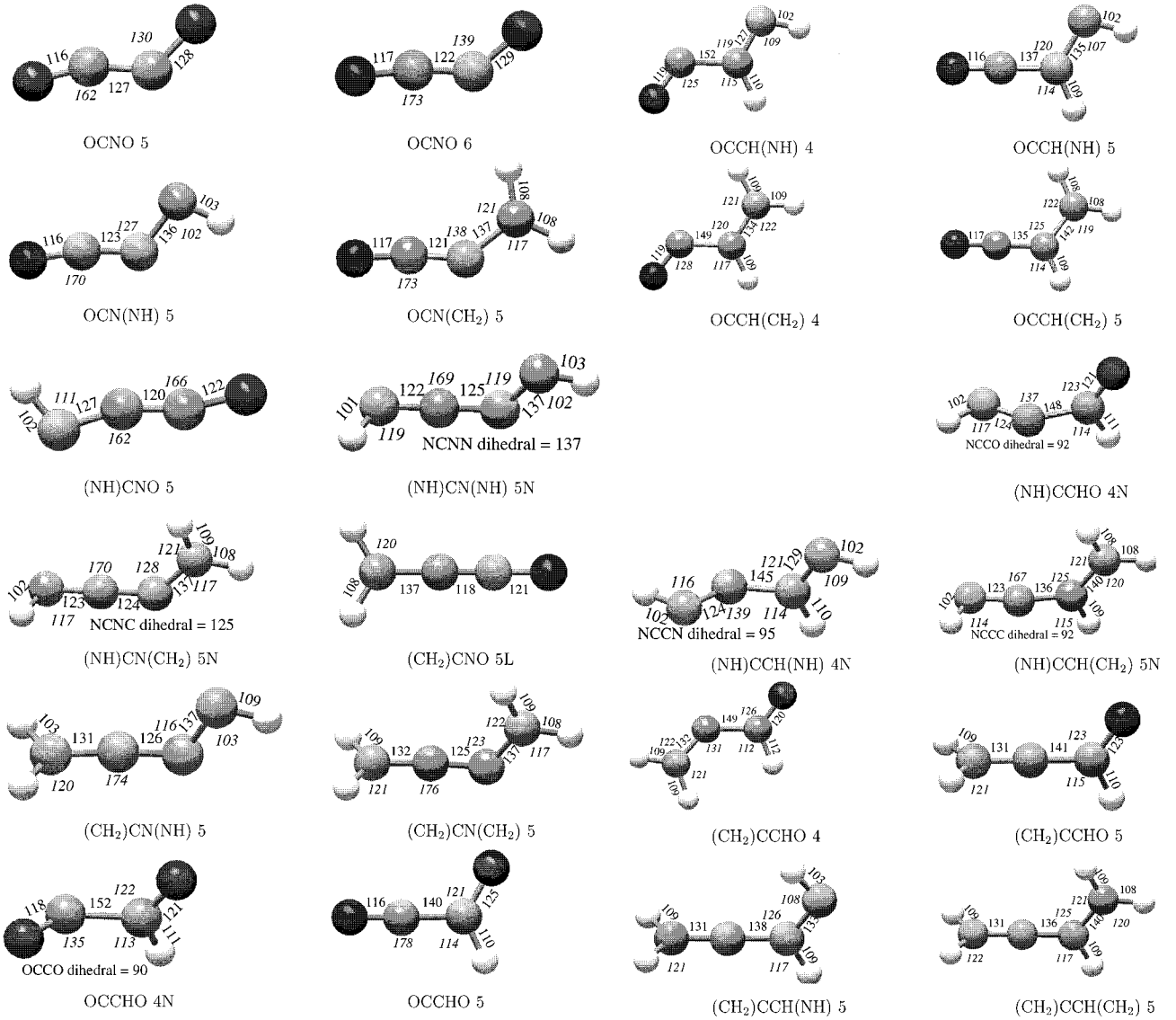

Figure 4. QCISD/6-311G(d,p) optimized geometries of XCNY and XCCHY local minima at 40 kJ mol^{-1} or below. Symmetry unique bond lengths are given in pm and angles (in italics) in degrees. Unmarked in-plane bond angles are 180°, and unmarked dihedral angles are 90°.

Configuration 5 is the most stable form of nearly everything else. The stability of 5 may be attributed largely to the allylic electron distribution of the CCY or CNY chains. This also serves to strengthen the central bond, which in configuration 4 is a formal single bond weakened by siphoning of electron density to the X and Y end groups. Configuration 5 is relatively stable for the OCCHY molecules, lying less than 10 kJ mol^{-1} above 4 at the QCISD levels, and being more stable than 4 by 2 to 15 kJ mol^{-1} at UHF.

A fairly reliable predictor of the 5−4 relative stability appears to be the sum of the UHF orbital energies for the unpaired electron orbital and the C−Y or N−Y π bond orbitals. These orbitals form the allylic system in configuration 5, so may be expected to exemplify any significant contribution of this system to the structural stability. Table 5 lists the differences between the energies of these three spin−orbitals for configurations 4 and 5, in other words:

$$\Delta E_{\mathrm{orb}} \equiv [E_4(\pi\alpha) + E_4(\pi\beta) + E_4(\mathrm{upe})] - [E_5(\pi\alpha) + E_5(\pi\beta) + E_5(\mathrm{upe})] \quad (1)$$

where $\pi\alpha$ indicates the α spin−orbital of the C−Y or N−Y π bond orbital, and "upe" indicates the unpaired electron orbital.

Table 5. ΔE_{orb} Values (hartree)

X/Y	CH_2	NH	O
	XCNY		
CH_2	−0.13	−0.36	−0.24
NH	0.11	0.10	0.07
O	0.05	0.05	0.05
	XCCHY		
CH_2	−0.26	−0.40	−0.35
NH	0.01	0.02	−0.02
O	−0.01	0.0	

Those entries for which this difference is greater than 0.05 hartree are found to be most stable as configuration 4, and the OCNYs (for which this value is 0.05) have nearly isoenergetic configurations 4 and 5.

Configuration 6 can be obtained by a linear XCNY chain with the nitrogen lone pair in a pure p-type MO. The energy cost of straightening the chain is offset by allylic stabilization in the other plane. Most of the XCNY configuration 6 optimized geometries have linear or near-linear CNY bond angles. Configuration 6 is found to lie less than 30 kJ mol^{-1} above the lowest energy configuration 5 for the OCNYs and for (NH)CN(CH_2). Configuration 6 geometries were not obtained

for (NH)CN(NH) or (CH_2)CNO because the configuration does not correspond to a stationary point, converging in either case without barrier to a more stable configuration.

Because straightening the backbone is not an option for the XCCHY species, configuration 6 does not appear to be a competitively low-energy form of those molecules. Unrestricted Hartree−Fock calculations predict only two of the XCCHY molecules to have a configuration 6 relative energy below 60 kJ mol^{-1}, the lowest being for OCCH(CH_2) and (NH)CCH-(CH_2). None of the XCCHY configuration 6 structures lie below 50 kJ mol^{-1} according to the QCISD calculations. Configuration 6 is generally unstable with respect to vibrational coordinates that couple the geometry to configuration 5, but is found to be a minimum on the QCISD surface in the cases of OCNO, OCCHO, and (CH_2)CNO.

3.3.2. OCNY. The three OCNY molecules are most stable as configuration 5. Configuration 4 is predicted to lie over 60 kJ mol^{-1} higher in energy for OCN(NH) and OCN(CH_2), and in the case of OCNO dissociates without barrier into CO and NO. Configuration 6 is significantly more stable than 4 in these three molecules, lying less than 30 kJ mol^{-1} above the ground state, while configuration 4 is predicted to lie at 58 kJ mol^{-1} or higher. However, OCNO appears to be alone among the XCNY series in having a vibrationally stable configuration 6.

The especially low relative energy of 6 in the case of OCN(CH_2) may be attributable to its linear OCNC backbone, for at this C_{2v} geometry the vibrational surface intersects that of configuration 5. Configuration 5 has a spin density highly localized on the methene carbon and bond lengths (1.21 Å for OC−NC, 1.37 Å for OCN−C) suggestive of a very strong central bond. These suggest a fairly weak contribution from the H_2C═N−C═O resonance structure and therefore an electron distribution similar to that associated with 6. Configurations 5 and 6 in this case may be regarded as minimum and saddle point conformations, respectively, of the same configuration.

The 5*a*″ and 6*a*″ potential energy surfaces also intersect for OCNO, this time at a linear geometry with a $^2\Pi$ electronic ground state. The Π state degeneracy is broken by the bending of the OCNO chain either in the plane of the unpaired electron orbital (leading to configuration 6) or perpendicular to that plane (leading to 5), in an example of the Renner−Teller effect.[36] In this case, deformation along either plane produces a more stable geometry than the linear $^2\Pi$ state because the N atom lone pair orbital may lie in either plane relative to the unpaired electron. Therefore, as the CNO bond angle bends to form either configuration 5 or 6, the N atom lone pair may be accommodated by an sp^2-type orbital, significantly more stable than the pure p-type orbital enforced by the linear geometry.

Of the radicals studied in the present survey, OCNO has been the subject of the most intensive computations to appear in the previous literature. Benson and Francisco carried out geometry optimizations, vibrational frequency analysis, and ΔH calculations of configuration 5 at levels of theory up to QCISD(T) with basis sets as large as 6-311G(2d,2p) for optimization and 6-311G(3df,3pd) for single-point energies.[8] The present work adds to this the investigation of the relative configurational energies and vibrational potential energy surface.

3.3.3. (NH)CNY. In changing the X substituent to NH from O, configuration 4 is somewhat stabilized, presumably because the diminished electronegativity of the nitrogen does not weaken the C−N central bond as significantly as oxygen. At the UHF level, (NH)CNO is a bound molecule in configuration 4 (unlike OCNO), but still lies more than 60 kJ mol^{-1} above the most stable configuration. Similarly, (NH)CN(NH) and (NH)CN(CH_2) have relative energies for configuration 4 some 20 kJ mol^{-1} lower than than the analogous Y equals O species.

Configuration 5 remains the most stable, although only the QCISD calculation of (NH)CNO yields a strictly C_s symmetry optimized geometry. In the other results, the NH bond twists out of the molecular plane to accommodate the in-plane NC π-bond. The constrained C_s geometry is not a local minimum for (NH)CN(NH) or (NH)CN(CH_2).

At the HF and QCISD levels, configuration 6 of (NH)CN-(CH_2) optimizes very nearly to the C_{2v} geometry it shares with 5, only some 25 kJ mol^{-1} above the twisted form of configuration 5. However, this form is unstable with respect to the two vibrational coordinates that couple it to the nonsymmetric geometry 5N: the methene rotation that will make the CN(CH_2) group planar, and the CNH bend that pushes the imine H atom out of the molecular plane.

3.3.4. (CH_2)CNY. A C_{2v} geometry is the global minimum energy structure of (CH_2)CNO. Indeed, a configuration 6 geometry is not obtained for (CH_2)CNO because any initial geometry similar to the canonical configuration 6 converges without barrier to this C_{2v} structure. The same holds for configuration 6 of (CH_2)CN(NH), although the C_{2v} structure in that case is not the global minimum.

The C_{2v} structures of (CH_2)CNO and (CH_2)CN(NH) are in fact distinct from the configurations so far discussed, and are labeled "5L" (5 for resting on the 5*a*″ surface, "L" for the linear backbone) in Table 4. In the HF and QCISD calculations, 5L is characterized by short C−N and N−O bond lengths (1.18 and 1.21−1.26 Å at QCISD), a long C−C bond (1.37 Å), little formal charge on the N atom, and the spin density almost wholly localized on the methene carbon atom. The corresponding configuration is $H_2C\cdot$ −C≡N═O, with a pentavalent nitrogen atom effectively back-donating electron density from its lone pair into the surrounding π bonds. Canonical bond lengths for the C≡N triple bond and N═O double bond are 1.16 and 1.22 Å, respectively, whereas the C═N double bond and N−O single bond are typically 1.32 and 1.41 Å.[37] This configuration is not possible when the two-coordinated N atom is replaced by the three-coordinated C atom in the XCCHY species below.

The C−N bond lengths in configuration 5 of (CH_2)CN(CH_2) and (CH_2)CN(NH) are about 1.26 Å, the CNY bond angle is about 120°, and the spin density has shifted to the terminal Y atom, all representative of the configuration 5 electron distribution drawn in Figure 1. The C_{2v} structure continues to be the most stable point on the 6a″ surface for these molecules, but lies some 50 kJ mol^{-1} or more above the configuration 5 minimum.

3.3.5. OCCHY. With the exception of the OCCH(CH_2) configuration 5 ROHF results, configurations 4 and 5 of all three OCCHY molecules are predicted to be stable in some form and to lie within about 15 kJ mol^{-1} of each other. The UHF results put configuration 5 slightly lower in energy, the ROHF and QCISD favor configuration 4. For OCCH(NH), the QCISD zero-point correction is sufficient to bring configuration 5 more stable than 4, but only by 1.5 kJ mol^{-1} (this is the sole case in the survey in which the QCISD energy ordering is affected by the zero-point correction).

The OCCH(CH_2) configurations 4 and 5 have been described previously;[9] there appear to be no previous studies of the OCCHO or OCCH(NH) radicals. At the UHF level, OCCHO

(36) Brown, J. M.; Jørgensen, F. *Adv. Chem. Phys.* **1983**, *52*, 117−180.

(37) Ladd, M. F. C.; Palmer, R. A. *Structure Determination by X-ray Crystallography;* Plenum Press: New York, 1985.

is at least 100 kJ mol^{-1} more stable than 15 other competing structural isomers. However, the radical is not readily formed from the parent $C_2H_2O_2$, glyoxal, because the glyoxal C−C bond, rather than the C−H bond, tends to cleave during photolysis and combustion.[38,39] Hartley[40] established a C−C bond strength of 299 kJ mol^{-1} for glyoxal, significantly lower than the typical aldehyde C−H bond strength of 365 kJ mol^{-1}. Previous calculations have been carried out by Langenberg and Ruttink[41] on the isoelectronic $C_2H_2O_2^+$ radical cation.

The barrier for isomerization of OCCHO configuration 5 to 4N was identified to be 5.2 kJ mol^{-1} at CISD and 1.0 kJ mol^{-1} at the QCISD level, with zero-point corrections in each case that remove the barrier entirely. The 3−4 kJ mol^{-1} well that remains centered on configuration 4N is deep enough to contain only three or four torsional states. Configuration 4N is predicted to be the only experimentally observable form of ground-state glyoxallyl, with vibration across the other configurational geometries becoming accessible at relatively low torsional excitation.

The OCCHO radical is one of only two XCCHY radicals in the survey found to be vibrationally stable in configuration 6, but the state nevertheless lies over 90 kJ mol^{-1} above the more stable configurations 4 and 5.

3.3.6. (NH)CCHY. In these three molecules, a nonplanar geometry is the most stable at UHF and QCISD levels, while configuration 4 is the most stable at ROHF. The nonplanar stable geometry of (NH)CCHO has been labeled "4N" in Table 4 because at the ROHF and QCISD levels this minimum strongly localizes the spin density on the CNH carbon (0.75 and 0.64 spin density for ROHF and QCISD, respectively), causing the CCN bond angle to bend to between 130° and 140°. The only nonplanar minimum identified at the UHF level, however, more closely resembles configuration 5, with the spin density divided between the oxygen and CNH carbon atom and with a weakly bent 170° CCN bond angle. The same qualitative result holds for (NH)CCH(NH), with the nonplanar geometry resembling configuration 4 at the QCISD level and 5 and the UHF level. However, for (NH)CCH(CH_2), the nonplanar QCISD geometry is more similar to 5, having a 167° NCC bond angle and spin density concentrated at the terminal carbon rather than the CNH carbon.

The quoted configuration 5 properties for these molecules are obtained from planar geometries, which force the N−H bond to lie unhappily in the plane of the backbone. This accounts for the particularly high configuration 5 energies given in Table 4 for these molecules when compared to the (CH_2)CCHY and OCCHY species. Excepting the ROHF calculation for (NH)CCHO 5 (which is a minimum), these calculations yield saddle point geometries with imaginary frequencies along the N−H out-of-plane bend. However, when the optimized planar geometry is slightly deformed in this direction, the geometry optimizes without fail to configuration 4N. This also occurs if the planar geometry is modified to fix the N−H dihedral to 90°.

At the QCISD level, each of the three molecules is found to be unstable in the planar-4 configuration with respect to the 4N configuration which lies 5−10 kJ mol^{-1} lower in energy. However, the planar-4 configuration is predicted to be vibrationally stable and even the global minimum in several of the HF calculations.

3.3.7. (CH_2)CCHY. Configurations 4 and 5 of (CH_2)CCHO[9] and (CH_2)CCH(CH_2)[7] have been discussed elsewhere, including limited analysis of the potential energy surfaces coupling configurations 4 and 5. Both configurations are found to be minima on the surface of the (CH_2)CCHO radical, and they correspond to acroleinyl and propenallyl radicals, respectively. Configuration 4, however, is predicted to have only a 1 kJ mol^{-1} barrier, less than the expected error in these relative energies and probably too small to confine a bound vibrational state in any case. The (CH_2)CCH(CH_2) butadienyl radical deforms spontaneously from configuration 4 (1,3-butadien-2-yl) to the allylic configuration 5 (1,2-butadien-3-yl). The principal addition from the present work is the consideration of configuration 6, which is vibrationally unstable with respect to 5 and lies some 55 kJ mol^{-1} higher in energy.

The (CH_2)CCH(NH) radical is formed by loss of a hydrogen atom from 1-aminopropadiene (configuration 5) or 3-iminopropene (configuration 4). Although both forms are stable at the HF levels, the QCISD predicts that 4 will deform without barrier to 5, as in the case of butadienyl.

4. Conclusions

Of the 18 radicals studied, five are predicted to have second configurational minima within 30 kJ mol^{-1} of the ground state, and all but (NH)CNO and (CH_2)CNO are predicted to have configurational saddle points within 50 kJ mol^{-1}. The presence of multiple minima on some of these surfaces indicates that photolysis or pyrolysis of corresponding parent compounds, processes which often leave a vibrational energy surfeit of 30 kJ mol^{-1} or more, may result in multiple isomers of the resulting reactive intermediates and branching of the subsequent chemistry. Qualitative features of the energy-ordering among these configurations may be justified by a combination of basic structural, electronegativity, and molecular orbital arguments.

One sees in this series early stages of a progression from chemical bond toward van der Waals bond dynamics. At relatively low vibrational excitation, for example, the vibrational states of the OCNO and OCCHO systems could likely be better modeled as OC−NO and OC−HCO hindered internal rotations rather than harmonic oscillator vibrations, in a manner analogous to typical treatments of the highly excited bending states of HCN.

The highest-level computations in the present work suggest superior results are obtained from single-reference CI calculations rather than low-level multireference methods in the description of these relocalization problems, and this is supported by comparisons to experimental results discussed elsewhere.[7,12] Agreement between single-reference and multireference methods was effected by extending the MCSCF calculations to incorporate all the valence electrons. Discrepancies found in earlier MCSCF analyses of the C_3H_3O and C_4H_5 molecular systems are therefore attributed to insufficient substitution of lower-energy valence electrons in the MCSCF calculations.

Several of these relative configurational energies are close enough to challenge the accuracy limits of ab initio calculations. Repeated tests reveal no evidence that the inclusion of triple CI substitutions or f-type basis functions substantially improve the relative configurational energies of these systems, although these have a clear impact on the dissociation energies. Given routine discrepancies of 30−50 kJ mol^{-1} between the Hartree−Fock and QCISD relative energies, HF results should be

(38) Zhu, L.; Kellis, D.; Ding, C.-F. *Chem. Phys. Lett.* **1996**, *257*, 487−491.
(39) Fletcher, R. A.; Pilcher, G. *Trans. Faraday Soc.* **1967**, *66*, 794−799.
(40) Hartley, D. B. *Chem. Commun.* **1967**, 1281−1282.
(41) Langenberg, J. H.; Ruttink, P. J. A. *Theor. Chim. Acta* **1993**, *85*, 285−303.

interpreted with caution when these significant electron redistributions occur.

Acknowledgment. Computational resources were provided largely through a cooperative agreement with the Compaq Corporation and by the Mississippi Center for Supercomputing Research. This work was funded in part by the National Science Foundation and the Petroleum Research Fund, administered by the ACS.

Supporting Information Available: A listing of QCISD vibrational data for the most stable isomers and OCCHO properties as functions of computational methodology (PDF). This material is available free of charge via the Internet at http://pubs.acs.org.

JA0037522